ISSN: 0067-2904

Theoretical Investigation of the Effects of some Geometrical Parameters on the Performance of Wire-Plate Electrostatic Precipitator

Wisam A. Latif [1], Mohammed O. Kadhim[1], Qays H. Ali[2]
[1]AL-Karkh University of Science, College of Energy and Environmental Science
[2]Ministry of Science and Technology, Baghdad, Iraq

Received: 2/1/2020 Accepted: 22/12/2020

Abstract

Some geometric parameters affecting the performance of a wire-plate electrostatic precipitator (ESP) are investigated theoretically. A numerical model was built to investigate the influence of the discharge wire size, wire separation, collector plates spacing, and roughness factor on the ESP performance. The results show that thinner wires emit higher current than larger ones at the same applied voltage, which would be suitable for low voltage power supply to generate the desired current density at the collecting electrodes. The results also show that, as the discharge electrodes get closer, the corona gets suppressed, resulting in a diminished corona current flow. On the other hand, as the distance between electrodes increases, the total current density decreases, leading to a less efficient ESP performance. Narrow spacing between collector plates gives a better performance. With regard to the effect of the roughness factor, the results revealed that the emitted current is strongly affected by the wires physical conditions.

Keywords: Electrostatic precipitators (ESP), ESP performance, ESP geometric parameters effects, ESP Numerical model.

دراسة نظرية لبعض المعلمات الهندسية المؤثرة في المرسبات الكهروستاتيكية

وسام علي اللطيف [1]، محمد الكاظم ، قيس حسن علي[2]
[1]كلية الطاقه وعلوم البيئة ، جامعة الكرخ للعلوم
وزارة العلوم والتكنولوجيا ، بغداد، العراق

الخلاصة

تم بحث بعض المعلمات الهندسية التي تؤثر على أداء المرسّبات الكهروستاتيكية (ESP) نظريًا. وقد تم بناء نموذج عددي للتحقيق في تأثير حجم سلك التفريغ والمسافة بين الأسلاك وتباعد الواح التجميع وعامل خشونة اسلاك التفريغ على أداء المرسبات الكهروستاتيكية. ظهرت النتائج أن الأسلاك النحيفة ينبعث منها تيار اعلى من التي أكبر حجما عند نفس الجهد المسلط والتي من شأنها أن تكون مناسبة لمجهزات قدرة واطئة وذلك لتوليد كثافة التيار المطلوب على اقطاب التجميع. واظهر النتائج أيضا أن اقتراب أقطاب التفريغ من بعضها يؤدي الى قمع الهالة (corona) مما يؤدي إلى انخفاض تدفق تيار الهالة. من ناحية أخرى، كما المسافة بين الأقطاب يزيد من انخفاض كثافة التيار الكلية مما يؤدي إلى تقليل كفاءة المرسبة اما تضييق المسافة بين الواح التجميع فيعطي أداء أفضل للمرسبة. وفيما يتعلق بأثر عامل الخشونة لأقطاب التفريغ بينت النتائج أن التيار المنبعث يتأثر بقوة مع الحالة الفيزيائية للإسلاك.

*Email: seniorqays@gmail.com

1. Introduction

Particulate matter emission is one of the main causes of air pollution, which has become increasingly hazardous to human health especially in developing countries. Systems such as settling chambers, bag filters, cyclones, wet scrubbers, and electrostatic precipitators have been widely used to control particulate emissions. The most promising of such systems are the electrostatic precipitators (ESPs), for their durability, high collection efficiency, and low operational cost. Thus, such promising device needs continuous study to achieve an optimum performance.

The basic operation principles of electrostatic precipitators are well described in the literature [1-4].

Several factors control the performance of electrostatic precipitators. Theoretical and experimental investigations on the parameters that have the most significant effects on the ESP performance, such as discharge wire size, wires separations, and collector plates spacing, have been carried out, but different conclusions were drawn in literature.

Abdel-Sattar and Singer [5], Chen and Wang [6] and Falaguasta *et al*. [7] concluded that higher efficiency is gained by using thinner wires, but Pontius, D. H., and Sparks, L. E. [8] and Yang et al. [9] showed that large size wires could improve the ESP performance. Al-Hamouz *et al*. [10] investigated the effect of wire size on the ESP power loss and showed that power loss increased with decreased wire size.

The effect of wire separations on the I-V characteristics was numerically studied by Lami *et al*. [11] and concluded that the maximum current increased with increasing wire separation, while Ruttanachot *et al*. [12] concluded that distance between wires had an insignificant influence on the ESP performance. Chen, G. J., and Wang, L. Q. [6] showed that shorter wire to wire distance provided better performance at various operating conditions. However, Arif *et al*. [13] concluded that reducing the wire separation resulted in a reduced total corona current due to increasing the degree of shielding. Also, they indicated that there should be a balance between the number of discharge wires and plate spacing to achieve the desired corona current.

Chang, C. L. and Bai, H. [14] indicated that large plate spacing offers high efficiency and high energy saving. On the other hand, Darby, k. [15] contradicted this conclusion due to the high power consumption that would be resulted with large plate spacing. Navarrete *et al*. [16] showed that a plate spacing of 400 mm was suitable for collecting high resistivity and 300 mm for the low resistivity materials. Nobrega *et al*. [17] studied the performance of a set of three precipitators and observed an increase in the performance as the gap between the collecting plates increased, leading to an increase in energy consumption per volume of cleaned gas. Ruttanachot *et al*. [12] and Arif *et al*. [13] demonstrated that the influence of the collection plate distance on the efficiency is greater than that of the wires spacing. Al-Hamouz *et al*. [10] concluded that reducing the gap between plates resulted in an increase in the corona power loss due to the reduction of the corona onset voltage.

The main reason for the diverse conclusions in investigating the various parameters affecting the performance of ESP is that different design criteria and operating conditions have been employed.

The present study presents a theoretical investigation of some geometric parameters affecting the performance of wire-plate ESP. These parameters are the discharge wire size, the wire separation, collector plates spacing, and the roughness factor.

2. Mathematical Formulations

The main systems of equations that relate the space charge distribution to potential or electric field distribution are the Poisson equation and the continuity equation:

$$\boldsymbol{\nabla^2 V} = -\frac{\rho}{\varepsilon_0} \tag{1}$$

$$\boldsymbol{\nabla . J} = 0 \tag{2}$$

$$\boldsymbol{E} = -\boldsymbol{\nabla}\, \boldsymbol{V} \quad (3)$$

$$\boldsymbol{J} = \rho b \boldsymbol{E} \quad (4)$$

where $\boldsymbol{V}$ is the potential, ρ is the total space charge density (ions charge density and the particle charge density), ε_0 is permittivity in a free space, b is the ion mobility, and $\boldsymbol{J}$ is the current density.

To solve equations 1-4 in two dimensions, a mathematical model based on the finite difference method was built, which is similar to that employed by McDonald *et al*. [18]. Figure 1 shows the flow chart of the program.

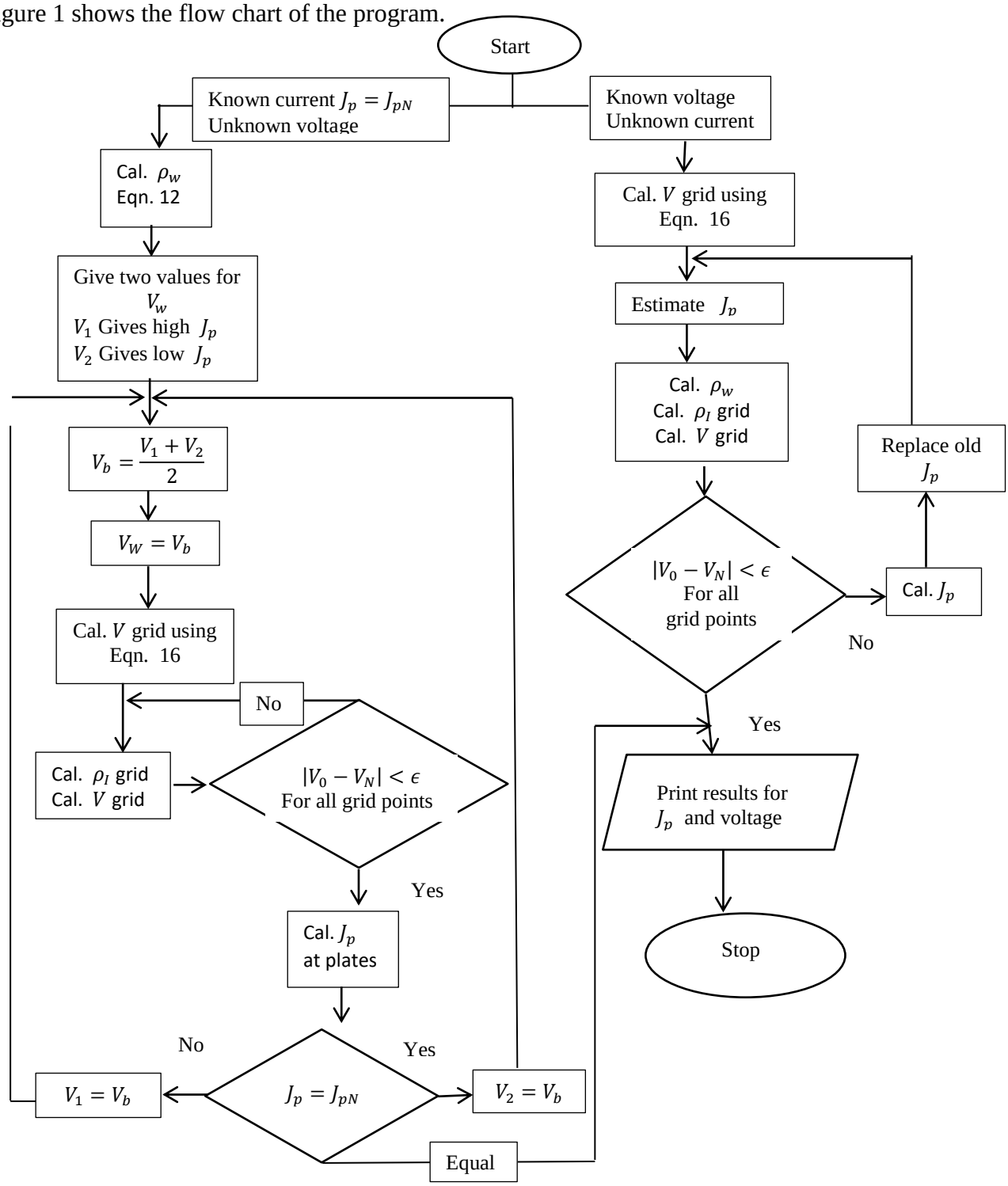

Figure 1- Flow chart for the program built to calculate the current- voltage characteristics in the wire-plate precipitator.

In order to find the solution for the electric field problem, the following assumption are required; the charged particles are uniformly distributed in the space between the collecting and discharged electrodes due to the turbulent action of the gas (gaseous medium that exist inside the precipitator, which includes air with percentages of CO, CO2, and gasses that result from fuel combustion). The turbulence is a result of the complex motion of the gas itself. The migration velocity of the particles is less than 0.3 m/s, which is small compared with the gas flow velocity. Therefore, the motion of these small particles is dominated by the turbulent motion of the gas stream [18]. Also the velocity of the ions is high enough so that they will not be uniformly distributed in the space between the collecting and discharge electrodes by the turbulent action of the gas.

The mathematical representation of Equation 1 in discrete form in two dimensions is

$$\frac{\partial^2 V}{\partial x^2} + \frac{\partial^2 V}{\partial y^2} = -\frac{\rho}{\varepsilon_0} \quad (5),$$

and the continuity Equation for current density (Equation 2), using vector algebra, can be expressed as:

$\boldsymbol{\nabla}.\boldsymbol{J} = \boldsymbol{\nabla}.(\rho b\boldsymbol{E}) = \rho b\boldsymbol{\nabla}.\boldsymbol{E} + b\boldsymbol{E}\boldsymbol{\nabla}\rho + \rho\boldsymbol{E}\nabla b = 0$,

where $\nabla.E = \frac{\rho}{\varepsilon_0}$ and $\nabla b = 0$ (assuming constant mobility of ions).

By substitution, the space charge will be

$$\rho = \left\{\varepsilon_0\left[E_x\frac{\partial \rho}{\partial x} + E_y\frac{\partial \rho}{\partial y}\right]\right\}^{1/2} \quad (6)$$

In solving the equations for V and ρ, the space charge zone is assumed to contain unipolar ions (no back-corona) [18].

The numerical representation for equation 5 is

$$V_{i,j} = \frac{1}{2(\Delta x^2+\Delta y^2)}\left\{\Delta x^2\left[(V_{i,j+1} + V_{i,j-1}\right] + \Delta y^2\left[V_{i+1,j} + V_{i-1,j}\right] + \frac{(\Delta x+\Delta y)^2}{\varepsilon_0}\rho_{i,j}\right\} \quad (7)$$

where

$\Delta x = x_{i+1} - x_i$

$\Delta y = y_{j+1} - y_j$

The charge density $\rho_{i,j}$ can be expressed using backward difference, which is suitable for the solution, since $\rho_{i+1,j}$ or $\rho_{i,j+1}$ are unknowns and have no first estimate.

$$\left.\frac{\partial \rho}{\partial x}\right|_{i,j} = \frac{1}{\Delta x}\left(\rho_{i,j} - \rho_{i-1,j}\right) \quad (8)$$

$$\left.\frac{\partial \rho}{\partial y}\right|_{i,j} = \frac{1}{\Delta y}\left(\rho_{i,j} - \rho_{i,j-1}\right) \quad (9)$$

Substituting equation 8 and 9 in equation 6 gives

$$\rho^2 - \varepsilon_0\left(\frac{E_x}{\Delta x} + \frac{E_y}{\Delta y}\right)\rho + \varepsilon_0\left(\frac{E_x}{\Delta x}\,\rho_{i-1,j} + \frac{E_y}{\Delta y}\,\rho_{i,j-1}\right) = 0 \quad (10)$$

Equation 10 is quadratic in ρ and can be solved to give

$\rho = -\alpha \mp (\alpha^2 + \beta)^{1/2}$ (11)

where

$$\alpha = \frac{\varepsilon_0}{2}\left(\frac{E_x}{\Delta x} + \frac{E_y}{\Delta y}\right)$$

$$\beta = \varepsilon_0\left(\frac{E_x}{\Delta x}\,\rho_{i-1,j} + \frac{E_y}{\Delta y}\,\rho_{i,j-1}\right)$$

Figure 2 represents a cross section in the precipitator configuration, showing the area of interest for which the governing equations are to be solved.

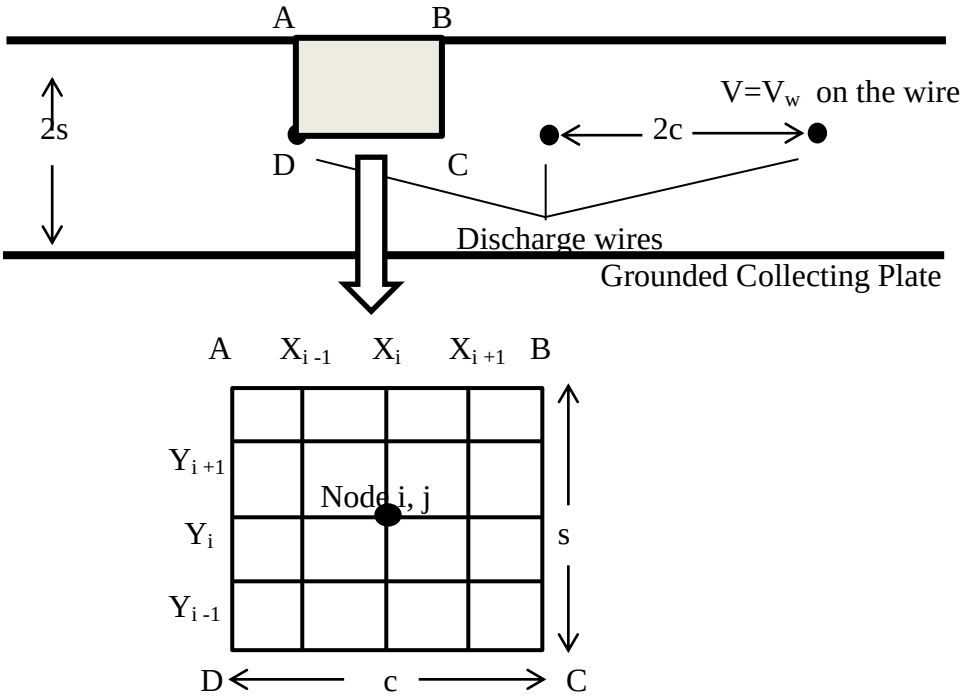

Figure 2- Cross section of wire-plate precipitator with nomenclature used in the numerical analysis.

Due to the symmetry around the wires, it is sufficient to study the area of the rectangle ABCD, asserting that the solution holds for all similar areas in the cross section, provided that symmetry is preserved.

2.1 Boundary conditions and solution procedures

The solution of Equations 7 and 11 is accomplished under the following boundary conditions (all the symbols used are illustrated in Figure 1):

1. $\rho = \rho_w$, at the wire (point D).
2. $E_x = E_y = 0$, at points C & D.
3. $V = 0$, at the plate (line AB).
4. $E_y = 0$, along line CD.
5. $E_x = 0$, along lines CB, BA, and AD.
6. $J = bE_y\rho$, near the plate.

The space charge density ρ_w near the wire at the edge of the corona, for a wide range of current densities and applied voltages, can be calculated from the following equation [18]

$$\rho_w = \frac{2CJ_p}{\pi b r_i E_i} \tag{12}$$

Where $C = 1 + \frac{2\lambda}{d}\left(1.257 + 0.40e^{\frac{-1.1\,d}{\lambda}}\right)$ is the Cunningham correction factor, with λ is the mean free path of gas molecular and *d* is the particle diameter [19], J_p is the current density at the plates, r_i is the radius of the ionized zone, and E_i is the electric field strength at the boundary of the ionized zone.

The product $r_i E_i$ can be determined by a common simplifying assumption [18]

$$r_i E_i = r_w E_c \tag{13}$$

where r_w is the radius of discharge wire and E_c is the electric field strength at the surface of the discharge wire, given by Peek's empirical formula [20]

$$E_c = 3.1 \times 10^6 F\delta\left(1 + 0.0308/\sqrt{\delta r_o}\right) \text{ V/m} \tag{14}$$

F is the discharge wire irregularity factor. $F = 1$ for clean polished wire.

δ is the relative air density = $2.98\frac{P}{T}$, P (in kPa) and T (in K) are the operating pressure and temperature. Also, the relative pressure = $\frac{P}{P_0}$ where P_0 is the atmospheric pressure. r_o is the radius of the corona zone and can be estimated from the following empirical Equation [21,22]

$$r_o = r_w + 0.03\sqrt{r_w} \tag{15}$$

Following the calculation of the value for the space charge near the wire, the generation of the first estimate for the potential grid is needed to generate the first space charge density grid using equation 10. The first potential grid is generated by Cooperman's electrostatic series which neglects the effect of space charge [23]

$$V_{(x,y)} = V_w \frac{\sum_{m=-\infty}^{\infty} ln\left[\frac{\cosh(\pi((x-2mc)/2s)-cos(\pi y/2s))}{\cosh(\pi((x-2mc)/2s)+cos(\pi y/2s))}\right]}{\sum_{m=-\infty}^{\infty} ln\left[\frac{cosh(\pi mc/s)-cos(\pi r_w/2s)}{cosh(\pi mc/2s)+cos(\pi r_w/2s)}\right]} \tag{16}$$

The second step of the solution is to use equations 7 and 10 to calculate the potential and space charge density grids alternately in an iterative scheme. Solution is obtained when the change between the value of V and its previous value is negligible and the calculated J_p equals or close to the value that was initially used in equation 12. To accelerate the solution of equations 7 and 10, a successive over relaxation method (SOR) [24] is used in such a way that equation 7 is rewritten as

$$V_{i,j}^{k+1} = V_{i,j}^{k} + \omega\left(V_{i,j}^{k+1} - V_{i,j}^{k}\right) \tag{17}$$

where k is the iteration number.

It was found that the optimum convergence is obtained at $1 < \omega < 2$ for all grid points. The best value for ω depends on the mesh size in x and y directions and on the boundaries of the problem.

2.2 Particulate charging

The electric field is calculated at every node in the divided area after solving equations 1 and 2. Therefore, the average field between the discharge wire and the surface of the plate is calculated by averaging the calculated values of the field in this region.

This value is given by integrating the field function numerically (Trapezoidal rule) along the normal line from the wire to the plate at equidistant places [24].

$$E_{av} = \frac{1}{L}\int_0^L E\, dL \tag{18}$$

2.3 Collection efficiency

The collection efficiency for the mono disperse particle is given by Deutsch-Anderson equation

$$\eta = 1 - exp\left(-\frac{A_c}{Q}\omega_{av}\right) \tag{19}$$

where ω_{av} is the average migration velocity (m/s), A_c is the total collection area (m^2), and Q is the volumetric flow rate (m^3/s).

In practice, the gas entering the precipitator contains different particle sizes and each size has its own concentration. The overall collection efficiency (η_{ovr}) is given by [25]

$$\eta_{ovr} = 1 - \frac{C_{outT}}{C_{inT}}, \tag{20}$$

C_{inT}, C_{outT} are the total input and output particle concentrations, respectively.

So, the efficiency for each particle size (d1) would be

$$\eta(d1) = 1 - \frac{C_{out}(d1)}{C_{in}(d1)} \tag{21}$$

Combining Equation 19-21 yields

$$\eta_{ovr} = 1 - \frac{1}{C_{inT}}\sum_{i=1}^{i=m} C_{in}(d_i)\, exp\left[-\frac{A_c}{Q}\omega_{av}(d_i)\right] \tag{22}$$

If the particles fit a mathematical model for distribution, such as log-normal, then $C_{in}(d_i) = n(d_i)\delta d$, where *n(d)* is a normalized function describing particle size distribution of that dust

$\eta_{ovr} = 1 - \frac{1}{C_{inT}} \sum_{i=1}^{i=m} n(d_i)\ exp\left[-\frac{A_c}{Q}\omega_{av}(d_i)\right]\ \delta d$, and if *n(d)* is continuous, then

$$\lim_{m\to\infty} \sum_{i=1}^{i=m} n(d_i)\ exp\left[-\frac{A_c}{Q}\omega_{av}(d_i)\right]\ \delta d = \int_{d1}^{d2} n(d)\ exp\left[-\frac{A_c}{Q}\omega_{av}(d)\right]\ dd$$

Therefore, the overall collection efficiency would be

$$\eta_{ovr} = 1 - \int_{d1}^{d2} n(d)\ exp\left[-\frac{A_c}{Q}\omega_{av}(d)\right]\ dd \quad (23)$$

Regarding the particle distribution inside the precipitator, it is calculated by dividing the whole area into small slices in the x- direction and dividing each slice into small parts in the y-direction (Figure 3).

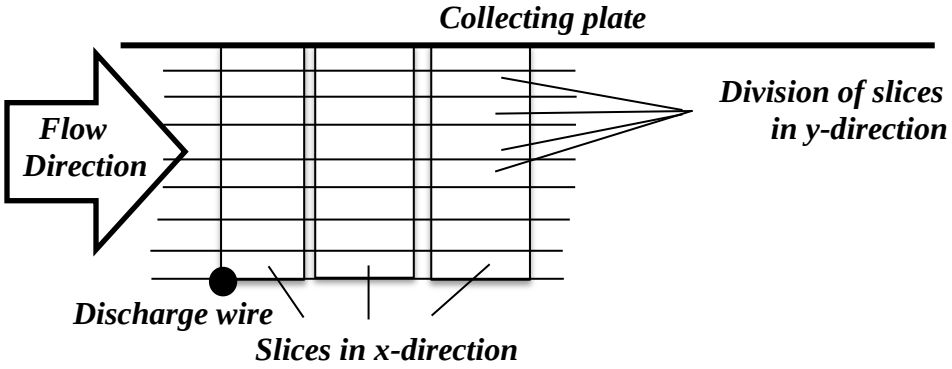

Figure 3- Partial section illustrating the division in x & y directions.

Each slice can be treated as a small precipitator with a length Δx and a width equals to half the distance between the plates. During their traveling from one slice to another, some of the charged particles will be precipitated on the collecting plates. The amount of precipitated particles depends on the value of electric field which is produced by solving Poisson's equation in each slice.

2.3 Model Validation

Prior to investigating the effects of the parameters on the ESP performance, the model is validated by comparing its results with published experimental data and field measurements. Figure 4 shows a comparison between the model prediction and the experimental data reported by McDonald *et al*. [18]. Clearly, the model prediction agrees fairly well with the experimental data. The value of the roughness factor is chosen to be 0.775 to reflect the condition of dirty wires used in the experiment.

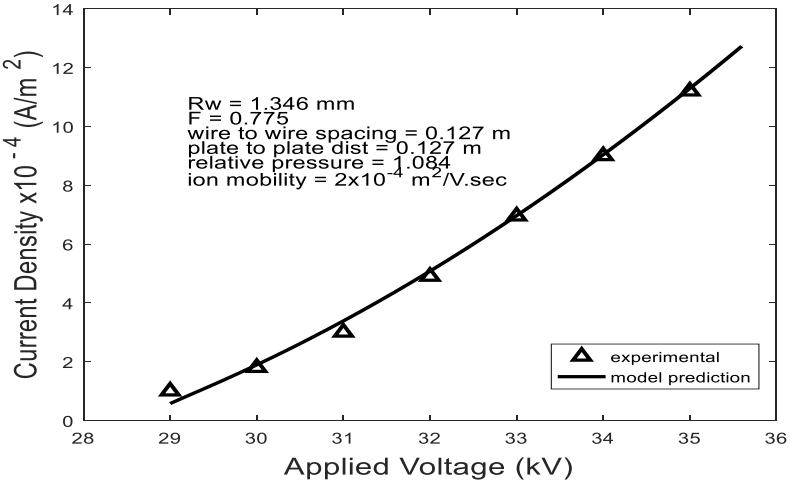

Figure 4-Comparison of the I-V characteristics between the model prediction and the experimental data reported by McDonald *et al*. [18].

Figure 5 illustrates a comparison of the calculated potential profiles, (a) along the line from the wire to the plate, and (b) from a point midway between wires to the plate for three different voltages and for the geometry used by Penney and Matick's experiment [26]. Again, the results show very good agreement with the experimental data.

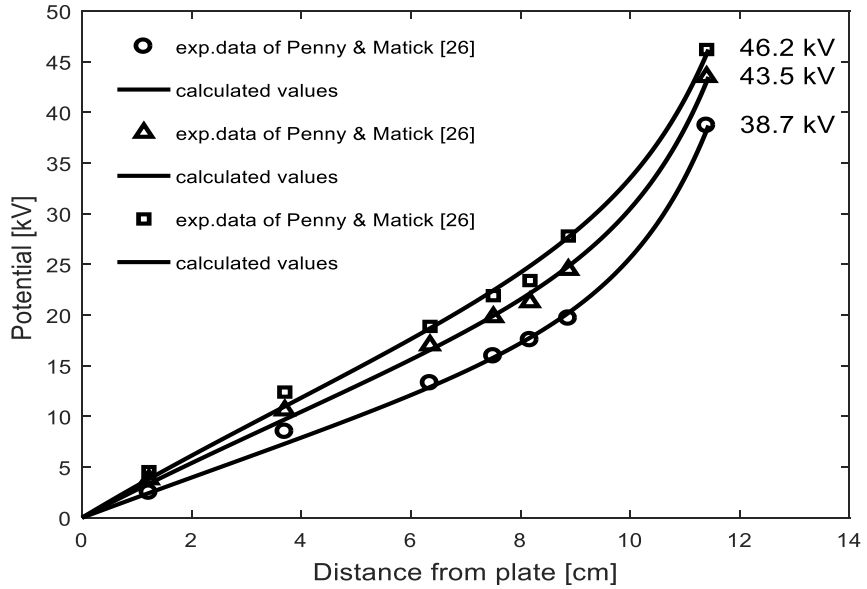

(a)

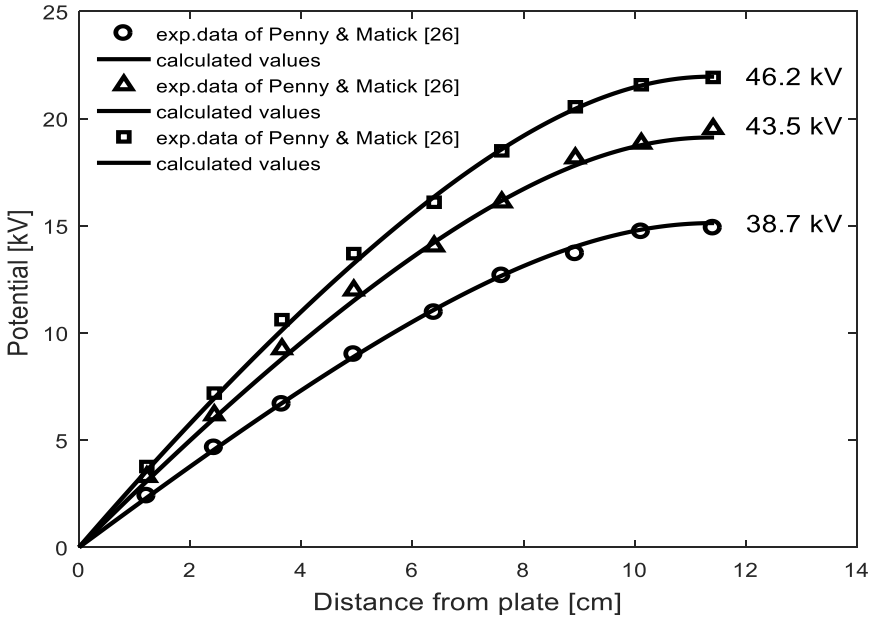

(b)

Figure 5-Model prediction for the potential distributions: a) along a line from wire to plate. b) along a line from a point midway between wires to plate for Penney & Matick [26] geometry, 2s = 228.6 mm, 2c = 152.4 mm, Rw = 1.016 mm, F = 1.

Figure 6 shows a comparison of the model prediction with the field measurement data of McCain *et al*. [27] for the fractional collection efficiency with respect to the particle size of a pilot-scale ESP. Once more, the model shows an acceptable agreement with experimental data.

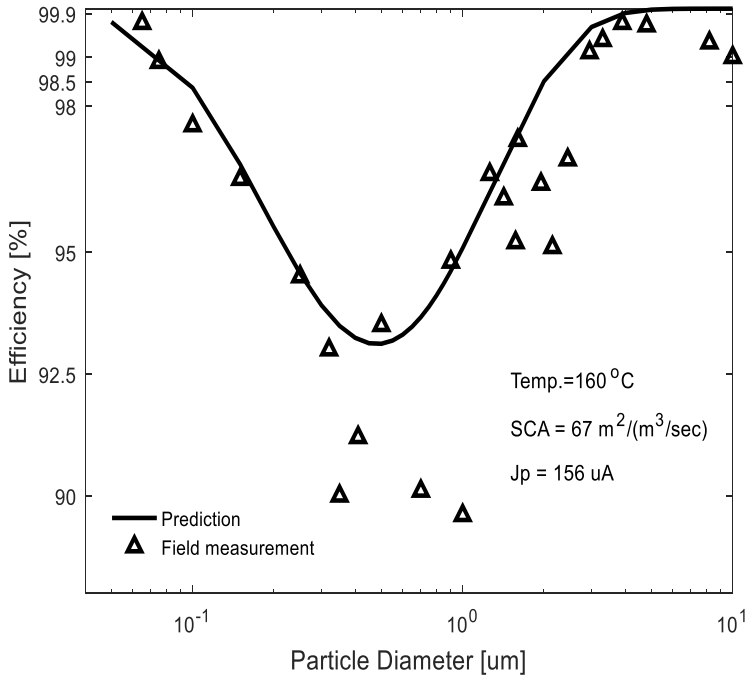

Figure 6- Prediction of the model for the fractional efficiency with respect to the particle size compared to the field measurement of McCain *et al*.[18] for an ESP on a pulverized coal boiler. The operating parameters are as indicated.

The experimental data show that the efficiencies of the particles with diameters larger than 4 μm tend to be less than the expected values. This is due to the re-entrainment of the collected dust and gas sneakage. Also, agglomeration rates for the 0.1 μm particles may have been very high during the time of measurement, resulting in under-estimating the collection efficiency [28]. This gives a reasonable explanation for the higher values obtained theoretically.

3. Results and Discussion

After its validation, the model was employed to investigate the effects of some geometric parameters on the performance of wire-plate electrostatic precipitator.

3.1 Effects of discharge wire size

Figure 7 shows the effects of the radius of the discharge wire on the I-V characteristics for the same ESP geometry used by McDonald *et al*. [18]. Clearly, smaller wire sizes could emit higher current than larger ones at the same applied voltage due to their lesser impedance. Thus, it can be concluded that wires with small diameters are suitable for low voltage power supply to generate the desired current density at the collecting electrodes. While larger wire size would be appropriate for large dimension precipitators where high voltages are needed at the discharge electrodes to induce the proper precipitating field at the collecting electrodes, with reasonable values for the current density.

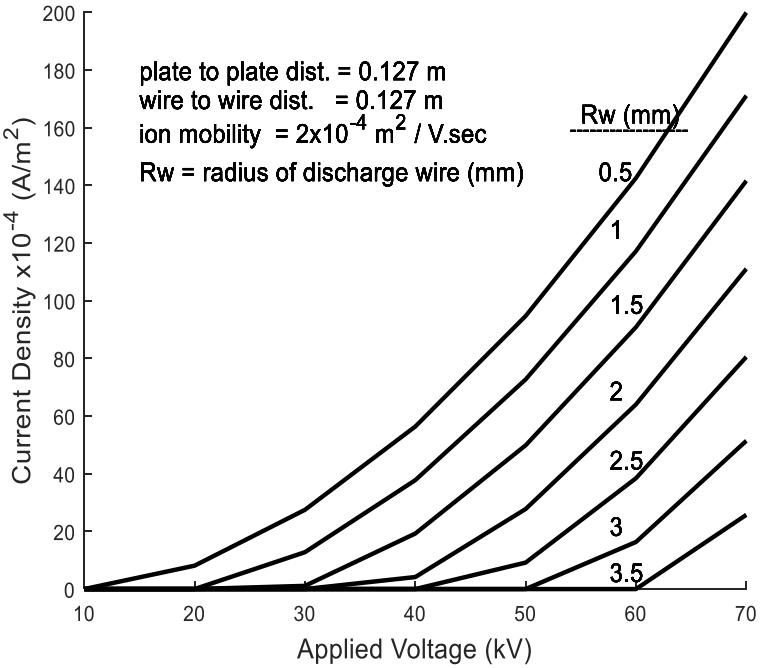

Figure 7-Theoretical calculations showing the effects of wire size on the I-V characteristics for the same ESP geometry used by McDonald *et al*.[18].

3.2 Effects of discharge wire separation

Keeping all the parameters and operation conditions constant and varying the wire separation (2c) from 10cm to 40cm, Figure 8(a) shows that, as the electrodes get closer the corona gets suppressed due to the distractive interference of the electric field lines, resulting in a diminished corona current flow. On the other hand, as the distance between electrodes increases, the total current density decreases, which greatly reduces the charging electric field. Ultimately, this leads to a less efficient ESP performance. Figure 8(b) shows that the optimum separation for maximum corona current is around 30 cm, which corresponds to 5 wires 30 cm apart. For the 50 and 60 cm separation, the number of wires was 3 and 2, respectively, which means that more power is needed to produce the required charging field.

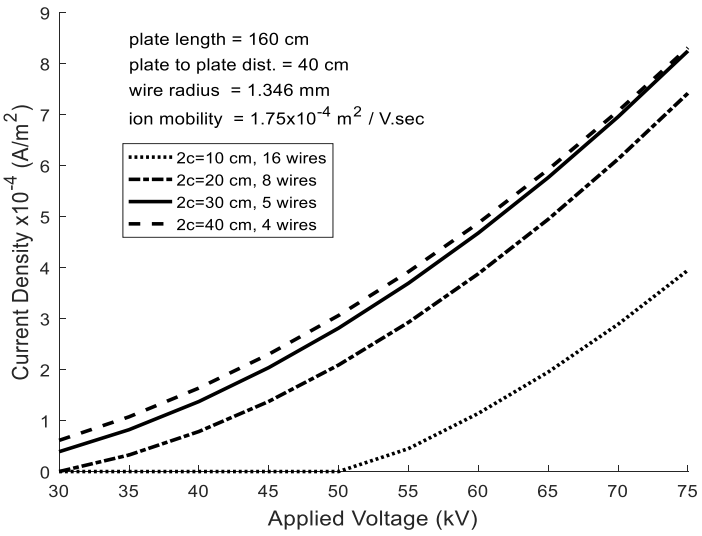

(a)

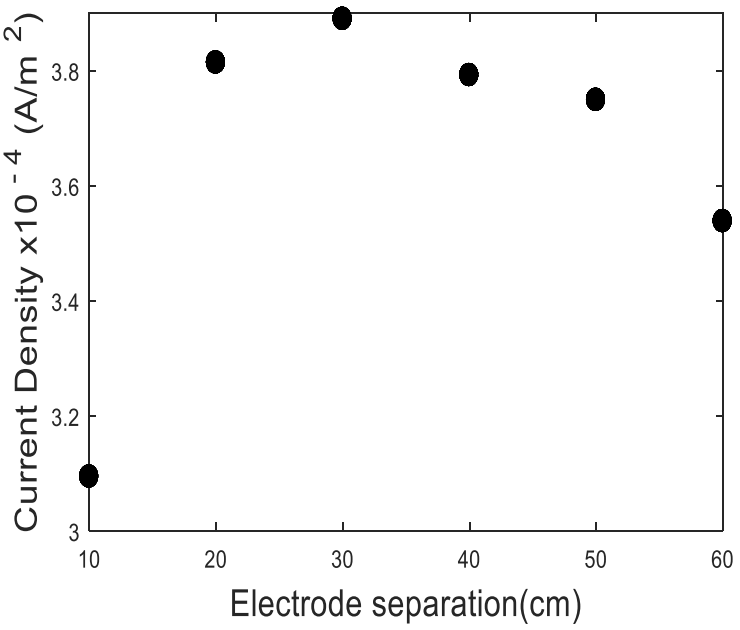

(b)

Figure 8- a) Effects of wire separation on I-V characteristics. b) Optimum wire separation for maximum corona current.

3.3 Effects of collecting plates spacing

Figure 9a illustrates the relation between the current density and the applied voltage for different collector plates spacing values. It can be seen that, as the plates get closer to each other, the current density gets higher at the same operating voltage. Thus, the narrow duct leads to strong electric field near discharge wire and the corona current will be easily generated.

Another way to evaluate the effects of the collector plate spacing is by comparing the precipitator efficiency for different duct widths at the same applied voltage. Figure 9b shows that all the curves have the same trend. The efficiency reaches minimum for particle size in the range of 0.4 μm. This is due to the fact that particle charging mechanisms can be divided into two types; ion bombardment, or field charging, and diffusion charging, where both types depend on the particle size.

The diffusion charging mechanism depends on collision between particles and ions which have random motion because of their thermal kinetic energy. Particle charging by this mechanism happens over the entire surface of the particle and requires a relatively long time to produce a limiting value of charge.

In ion bombardment charging, the particle accumulates charge by intercepting molecular ions. As the particle gains charge by capturing more ions, its own electric potential increases in magnitude and ultimately stops when the mean surface electrical potential of the particle is just equal to the mean kinetic energy of the ions at that point in the flow.

The diffusion charging is the main mechanism for charging submicron particles (less than 0.1 μm), while larger particles (greater than 1 μm) are charged by ion bombardment, leaving the size range between about 0.1 μm – 1 μm with no clear theoretical description [28]. It is observed form the figure that better performance is obtained for narrow spacing. This is because the increase in spacing between the collector plates requires more power to induce a field that is enough to provide the particles with the required migration velocity to reach the collecting plates.

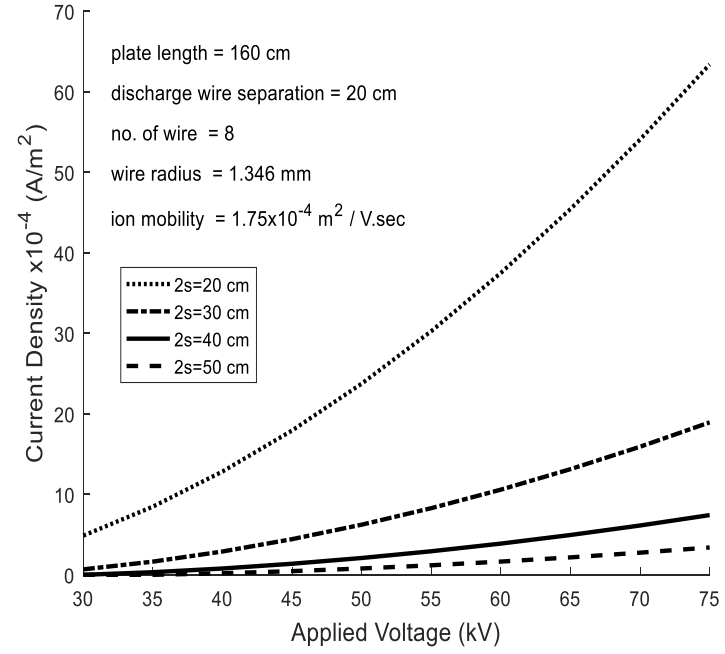

(a)

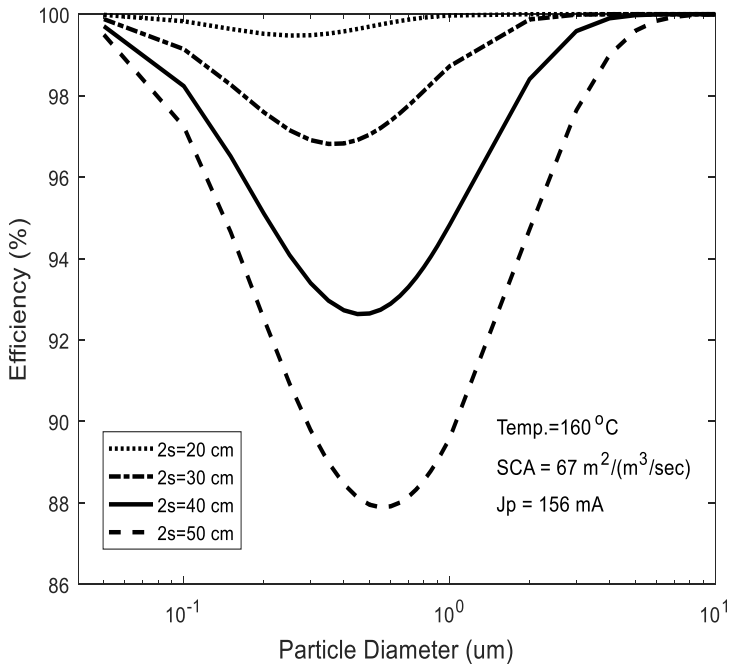

(b)

Figure 9-Model prediction for the effects of collecting plate spacing on a) I-V characteristics, b) ESP efficiency, keeping the same parameters used to obtain Figure 6.

From Figures 8a and 9a it is clear that the effects of wire separation on the current density and ultimately on the efficiency is less significant than the effects of plate spacing.

3.4 Effects of roughness factor (F)

The roughness factor of the discharge wire reflects its physical surface condition. This parameter has not been given, in literature, the attention that corresponds to its importance to the ESP performance. Figure 10 illustrates the theoretical calculation of the I-V characteristics of the same geometry used by McDonald *et al*. [18], with different values of

the roughness factor for the corona electrodes. It is evident that I-V characteristics are strongly affected by the wire condition, as the current emitted increases with deterioration of the discharge wire surface due to an increase of wire impedance, which leads to a wider corona zone. The deterioration of the wire is a result of the deposited dust, heat, and the ion or particles bombardment on the outer surface of the wire which produces scratched surface, causing a reduction in the value of the roughness factor.

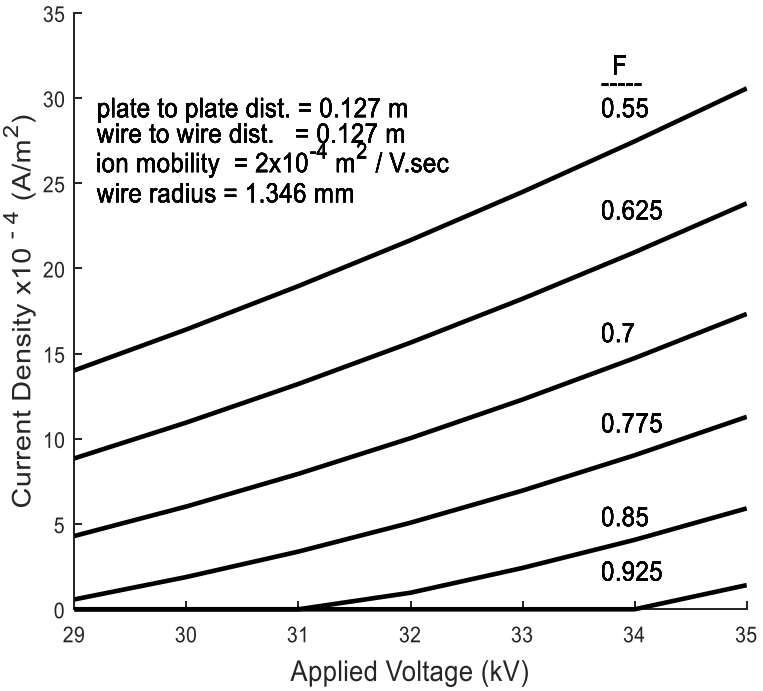

Figure 10-Theoretical calculations showing the effects of the roughness factor of corona wire on the I-V characteristics for the same ESP geometry used by McDonald *et al*. [18]

Conclusions

Some geometric design parameters affecting the performance of wire-plate electrostatic precipitator were theoretically investigated in this study by employing a numerical model, which showed a good agreement with published experiment data and field measurements. The study demonstrated that better ESP performance is obtained with thin discharge wires with an optimum wire separation that is fairly close to half the duct width. Also, the narrow duct offers strong electric field near discharge wire, which leads to greater efficiency. Moreover, it is concluded that plate spacing has a stronger effect than wire separation on the current density and ultimately on the efficiency.

The investigation showed that I-V characteristics were strongly affected by the wire physical condition, as the current emitted increased with the increase in time, due the deterioration of the outer surface of the wire, which produced scratched surface.

REFERENCES

[1] White, H. J. *Industrial electrostatic precipitation. Reading MA. Addison-Wesley*, 1963.

[2] Rose, H. E. and Wood, A. J. *An introduction to electrostatic precipitators. 2nd Ed, London, Constable*, 1966.

[3] Robinson, M. *Electrostatic precipitation. In: Strauss, W. (eds). Air Pollution Control-Part 1: New York, NY. Wiley-Interscience*, 1971.

[4] Benites, J. *Process Engineering and design for air pollution control. Englewood Cliffs, NJ: PTR Prentice Hall*, 1993.

[5] S. Abdel-Satar, S. and Singer, H. "Electrical conditions in wire-duct electrostatic precipitators". *J. Electrostatics*. vol. 26, pp. 1-20, 1991.

[6] Chang, C. L.; Bai, H. **"**Effects of Some Geometric Parameters on the Electrostatic Precipitator Efficiency at Different Operation Indexes". *Aerosol Science and Technology*, vol. 33, pp. 228-238, 2000.

[7] Falaguasta, M. C. R., Steffens, J., Valdes, E. E., Coury, J. R. "Overall collection efficiency of a plate-wire electrostatic precipitator operating on the removal of PM2". *Latin American Applied Research*, vol. 38, pp. 179-186, 2008.

[8] Pontius, D. H., Sparks, L. E. "Effect of Wire Diameter on Particle Charging and Collection Efficiency in Electrostatic Precipitators", Proc. 2nd Inter. *Conf. on Electrostatic Precipitation, Kyoto, Japan, Air Pollution Control Assoc*, 269–274, 1984.

[9] Yang, Xiu-feng., Kang, Yang-ming., Ke Zhang "Effects of geometric parameters and electric indexes on the performance of laboratory-scale electrostatic precipitators". *J. of Hazardous Materials*, vol. 169, no. 1-3, pp. 941-947, 2009.

[10] Al-Hamouz, Z., El-Hamouz, A., Abuzaid, N. "Simulation and experimental studies of corona power loss in a dust loaded wire-duct electrostatic precipitator". *Advanced Powder Technology*, vol. 22, pp. 706–714, 2011.

[11] Lami, E., Mattachini, F., Gallimberti, I., Turri, R., Tromboni, U. "Numerical procedure for computing the voltage current characteristics in ESP configuration". *J. of electronics*, vol. 34, vol. 4, pp. 385-399, 1995.

[12] Ruttanachot, C., Tirawanichakul, Y., Tekasakul, P. "Application of Electrostatic Precipitator in Collection of Smoke Aerosol Particles from Wood Combustion". Aerosol and Air Quality Research, vol. 11, pp. 90–98, 2011.

[13] Arif, S., Branken, D.J., Everson, R.C., Neomagus, H.W.J.P., Arif, A. "The influence of design parameters on the occurrence of shielding in multi-electrode ESPs and its effect on performance". *J. of electrostatics*, vol. 93, pp. 17-30, 2018.

[14] Chen, G. J.and Wang, L. Q. "The Research and Application of Electrostatic Precipitator with Wide Spacing and Cross-Positioned Channel Collecting Plates in the Power Plant", Proc. *2nd Inter. Conf. on Electrostatic Precipitation, Kyoto, Japan, Air Pollution Control Assoc*, pp. 362–367, 1984.

[15] Darby, K. "Plate Spacing Effect on Precipitator Performance", *Proc. 2nd. Inter. Conf. on Electrostatic Precipitation, Kyoto, Japan, Air Pollution Control Assoc*, pp. 376–383, 1984.

[16] Navarrete, B., Canadas, L.; Cortes, V., Salvador, L., Galindo, J. "Influence of Plate Spacing and Ash Resistivity on the Efficiency of Electrostatic Precipitators", *J. of Electrostatics*. vol. 39, pp. 65–81, 1997.

[17] Nobrega, S. W., Falaguasta, M. C. R., Coury, J. R. "A study of a wire-plate electrostatic precipitator operating in the removal of polydispersed particles", *Brazilian Journal of Chemical Engineering*, vol. 21, no. 2, pp. 275 – 284, 2004.

[18] McDonald, J. R., Smith, W. B., Spencer, H. W., Sparks, L.E. "A Mathematical Model for Calculating Electrical Conditions in Wire-duct Electrostatic Precipitation Devices". *J. Appl. Phys*. vol 48, pp. 2231–2243, 1977.

[19] Davies, C. N. "Definite Equation for the fluid resistance of spheres" (*Published Conference Proceedings style*), *in Proc. Phys. Soc*. vol. 57, no. 4, pp. 18, 1954.

[20] Peek, F. W. *Dielectric Phenomena in High-Voltage Engineering; 3rd ed. New York. McGraw-Hill*, 1929.

[21] Kallio, G. A., Stock, D. E. "Computation of electrical conditions inside wire-duct electrostatic precipitators using a combined finite element, finite difference method", *J. Appl. Phys*. vol. 59, pp. 1799-1806, 1986.

[22] Lami, E., Mattachini, F., Sala, R., Vigl, H. "A mathematical model of electrostatic field in wires–plate electrostatic precipitators", *J. Electrostatic*., vol. 39, no. 1, pp. 1-21, 1997.

[23] Cooperman, P. A. "Theory for space charge limited currents with application to electrical precipitation". *AIEE Trans*, pp. 47-50, 1960.

[24] Steven, S. Karris. Numerical Analysis Using MATLAB and Excel. 3rd. ed. London, Orchard Publications, 2007.

[25] Cristina, S. and Feliziani, M. "Calculation of ionized fields in DC electrostatic precipitators in the presence of dust and electric wind", *IEEE Trans., Ind. Appl*., vol. 31, pp. 1446-1451, 1995.

[26] Penney, G. W. and Matick, R. E. "Potentials in D-C corona fields", *Trans. AIEE*., vol. 79, pp. 91-99, 1960.

[27] McCain, J. C., Gooch, J., Smith, W. B. "Results of Field Measurements of Industrial Particulate Sources and Electrostatic Precipitator Performance". *J. Air Poll. Cont. Assoc*., vol. 25, pp. 117-121, 1975.

[28] Parasram, Navin Tarun. *Particle motion in electrostatic precipitators. PhD thesis, University of London. UK*, 2001.